Journal of Magnetic Resonance 208 (2011) 122–127

Contents lists available at ScienceDirect

Journal of Magnetic Resonance

journal homepage: www.elsevier.com/locate/jmr

Homonuclear mixing sequences for perdeuterated proteins

Kuo-Ying Huang, Ansgar B. Siemer *, Ann E. McDermott *

Department of Chemistry MC3113, Columbia University, 3000 Broadway, New York, NY 10027, USA

ARTICLE INFO

Article history:
Received 15 July 2010
Revised 18 October 2010
Available online 26 October 2010

Keywords:
Solid-state NMR
Homonuclear mixing
Perdeuteration

ABSTRACT

We tested the performance of several ^{13}C homonuclear mixing sequences on perdeuterated microcrystalline ubiquitin. All sequences were applied without ^{1}H decoupling and at relatively low MAS frequencies. We found that RFDR gave the highest overall transfer efficiency and that DREAM performs surprisingly well under these conditions being twice as efficient in the aliphatic region of the spectrum than the other mixing sequences tested.

1. Introduction

^{2}H isotope labeling (perdeuteration) is an established technique in protein liquid-state NMR and its great potential for solid-state NMR has been demonstrated by several studies in the last decade [1–5]. Most important for solid-state NMR is that perdeuteration leads to narrow ^{1}H linewidths of the remaining protons, which enables high resolution spectroscopy of this important nucleus. Furthermore, high-power ^{1}H decoupling becomes unnecessary in perdeuterated samples and low power liquid-state NMR type pulse sequences become applicable. However, perdeuteration also comes at a price. The gain in signal-to-noise ratio (S/N) due to ^{1}H–^{13}C cross polarization (CP) is reduced or absent. In the latter case, direct excitation of the ^{13}C spins using a 90° pulse instead of a CP can be preferred. The spin–lattice relaxation time T_1 of ^{1}H and ^{13}C alike can become quite long in perdeuterated samples. This problem can be overcome by adding paramagnetic centers that shorten the T_1 [6]. A third aspect is that a dense proton network, which is absent in perdeuterated samples, is a key instrument facilitating ^{13}C–^{13}C polarization transfer in many pulse sequences, such as proton driven spin diffusion (PDSD) [7], dipolar-assisted rotational resonance (DARR) [8], mixed rotational and rotary resonance (MIRROR) [9], or proton assisted recoupling (PAR) [10]. In the light of this last point, it becomes necessary to either re-evaluate the homonuclear mixing sequences previously developed for fully protonated systems or to find new techniques that replace PDSD and DARR.

Several recent papers illustrate successful recoupling of carbons in perdeuterated proteins. In one study, radio-frequency-driven recoupling (RFDR) was carried out with sample spinning at 20 kHz and a field of 800 MHz to obtain broadband recoupling on a 95% perdeuterated sample of microcrystalline ubiquitin, (with labile hydrogens exchanged with protonated solvent) [11]. Agarwal and Reif used an adiabatic TOBSY (total though-bond correlation spectroscopy) sequence with sample spinning at 20 kHz and a magnetic field of 600 MHz and achieved broadband ^{13}C mixing on perdeuterated SH3 crystals in the context of a 3D HCCH experiment. In their sample, only 10% of the labile protons exchanged back to ^{1}H [12]. Recently, Akbey and co-workers proposed a new pulse sequence called DONER. Similar to DARR, this sequence recouples protons and deuterons at the rotary resonance condition during the ^{13}C–^{13}C mixing. DONER spectra recorded on perdeuterated SH3 crystals (40% of the protons exchanged back) at 10 kHz MAS and a ^{1}H Larmor frequency of 400 MHz led to much higher transfer efficiency as compared to DARR or PDSD [13]. However, no comparative study has been done comparing the efficiency of these pulse sequences for perdeuterated samples.

In the present study, we try to determine the optimal homonuclear mixing sequence by comparing such mixing sequences namely RFDR, TOBSY, adiabatic TOBSY, SPC5, DREAM, DARR, DONER, and PDSD in perdeuterated microcrystalline ubiquitin. In the absence of strong proton couplings, many of these pulse sequences lead to high transfer efficiencies at low MAS frequencies without the need of any ^{1}H decoupling as illustrated below.

Many homonuclear mixing sequences have been developed (for recent reviews see Ref. [14]). A key in developing homonuclear mixing sequences has been good performance, despite the presence of strong ^{1}H–^{13}C and ^{1}H–^{1}H couplings. On the other hand, theoretical descriptions and numerical simulations of homonuclear recoupling sequences often assume perfect ^{1}H decoupling,

* Corresponding authors. Address: Columbia University, Department of Chemistry MC3132, New York, NY 10027, USA. Fax: +1 212 932 1289 (A.B. Siemer). Fax: +1 212 932 1289 (A.E. McDermott).

E-mail addresses: as3211@columbia.edu (A.B. Siemer), aem5@columbia.edu (A.E. McDermott).

1090-7807/$ - see front matter © 2010 Elsevier Inc. All rights reserved.
doi:10.1016/j.jmr.2010.10.015

neglecting all parts of the Hamiltonian involving proton spins [15–17]. Experimentally, efficient ^{1}H decoupling during ^{13}C recoupling is non-trivial and should be optimized with care [18,19]. In perdeuterated systems *i.e.* in the absence of ^{1}H–^{13}C couplings, homonuclear mixing sequences are expected to behave more closely to the numerical and theoretical predictions that assume perfect ^{1}H decoupling. One of the oldest sequences is RFDR, in which one 180° pulse per rotor period restores ^{13}C homonuclear dipolar couplings, which would otherwise be averaged by MAS [20]. RFDR and variants of this pulse sequences are still widely used. Another class of mixing sequences is based on windowless phase-modulated radio frequency pulse trains, which are known as C and R sequences [21,22]. These sequences can be used to recouple different parts of the Hamiltonian; for example the $C7^1_2$ (C7) or super cycled $C5^1_2$ (known as SPC5) sequence are popular sequences that restore homonuclear dipolar couplings [15,16]. Other C and R sequences introduce the full *J*-coupling Hamiltonian, including for example the TOBSY sequence [23,24]. This pulse sequence, which is similar to the TOCSY sequence in liquid-state NMR, and its adiabatic variants [25,26], have proven to be very efficient. Another class of recoupling sequences is based on non phase modulated spin-lock fields. For example, the DREAM sequence, an adiabatic amplitude sweep through the HORROR condition ($\omega_1 = 1/2\ \omega_r$; where ω_1 is the spin-lock field strength and ω_r the MAS frequency), gives very high transfer efficiencies [27,28]. However, due to the restriction in rf-field, DREAM is better suited for high MAS frequencies [29,30].

For protonated systems, all of these mixing sequences were shown to depend heavily on efficient ^{1}H decoupling during the mixing and detection periods. The need for strong decoupling can limit their efficiency, and lead to stresses on the probe and the sample. One successful class of experiments obviates the need for high power decoupling by applying high MAS frequencies with low power ^{1}H decoupling [30,31]. Fast MAS also has other advantages, for example suppression of CSAs at high magnetic fields. However, better averaging of dipolar couplings at fast MAS posed a different problems to spin diffusion based pulse sequences, which has been partly addressed by recently developed efficient recoupling schemes such as PAR or MIRROR. A second solution to the stress of high-power proton decoupling is to reduce rf-induced sample heating by using modern probes that dramatically lower the E-field inside the coil and thereby prevent sample heating [32,33]. A third approach to avoiding the damage due to high-power ^{1}H decoupling involves high ^{13}C recoupling rf-field strengths such as CMAR [34], R-TOBSY [35], and Post-$C20^3_6$ [36]. These recoupling sequences were shown to work even without ^{1}H decoupling, but either require relatively fast MAS frequencies (CMAR, R-TOBSY), or are less efficient than similar sequences with high-power ^{1}H decoupling (Post-$C20^3_6$). Finally, another very convenient solution to this problem is sample perdeuteration, since no ^{1}H decoupling is presumably necessary in the absence of protons. However, most known homonuclear mixing sequences were developed to perform under strong heteronuclear ^{1}H couplings. The present manuscript evaluates the performance of these sequences on perdeuterated ubiquitin, since heteronuclear couplings are absent in perdeuterated samples.

2. Results and discussion

To compare the transfer efficiency of different homonuclear mixing sequences, we recorded a series of 2D ^{13}C–^{13}C correlation spectra on ^{2}H–^{13}C–^{15}N labeled, human ubiquitin, which was crystallized from a fully protonated buffer. Considering that the sample was perdeuterated except of the back-exchanged amid protons, the ^{1}H–^{13}C CP at the beginning of all 2D spectra transferred mostly magnetization to C′ and Cα. Fig. 1 shows the results we got for the RFDR, DONER, DREAM, and adiabatic TOBSY (aTOBSY) sequences. All spectra were recorded under essentially the same conditions *i.e.* on a 400 MHz spectrometer, at 8 kHz MAS (8.333 kHz for aTOBSY) and with neither proton nor deuterium decoupling during t_1, t_2, and the mixing time. The complete absence of decoupling made all these sequences easy to set up as compared to protonated samples were the careful optimization of ^{1}H decoupling is often essential to obtain acceptable transfer efficiencies. The MAS frequencies of 8 and 8.333 kHz were chosen to avoid the C′–Cα rotational resonance condition at about 11.5 kHz. (Spinning above all rotational resonance conditions was not practical using a standard 4 mm setup.) The 8.333 kHz made sense in the case of the C and R type sequences such as aTOBSY, since it led to even pulse lengths. Except for DREAM and SPC5, all mixing sequence were optimized by dephasing the C′ line and observing of the magnetization buildup over time. (Typical 1D time arrays used to determine the mixing time are shown in Supplemental Fig. 1.) For DONER and DARR, we used the same mixing time (50 ms) as Akbey and co-workers under very similar conditions. This mixing time is also close to the optimal mixing time in the 1D time arrays. For RFDR, we used a slightly longer mixing time (3 ms) than for the maximal C′ intensity as a good compromise between transfer within the aliphatic region of the spectrum and transfer to C′, and also to achieve a good balance between one- and two-bond transfers (see Supplemental Fig. 2). For aTOBSY, we picked the mixing time (4.3 ms) that gave the best compromise between transfer and magnetization decay. DREAM and SPC5 were optimized by the maximum in the negative signals from the double quantum transfer (2 ms and 1 ms, respectively). These mixing times are good compromises between transfer within the entire aliphatic region of the spectrum and the overall polarization decay.

Generally, the homonuclear mixing sequences show similar recoupling patterns (*i.e.* relative cross peak intensities) on our perdeuterated sample as on comparable protonated samples under high-power ^{1}H decoupling. Except for the DREAM sequence, all recoupling techniques gave strong Cα–C′ correlations and less intense cross peaks in the aliphatic region of the spectrum. This behavior is expected for broadband recoupling sequences, since they do not lead to equal distribution of magnetization, but rather to a magnetization maximum at the end of the carbon chain (*e.g.* the carbonyl of peptides) [16].

The DREAM sequence on the other hand, generated more and stronger cross peaks within the aliphatic region (*e.g.* Cα–Cβ) as compared to RFDR, DONER, and aTOBSY spectra. At 8 kHz MAS, the HORROR condition is at the relatively weak spin-lock field of 4 kHz leading to a more band selective recoupling. However, even with this low spin-lock field we observed Cα–C′ cross peaks *i.e.* correlation between resonance ~11.5 kHz apart.

To quantify the transfer efficiency, we integrated the intensity of all cross peaks at the δ_1 slice at 54 ppm shown in Fig. 1 and of the additional PDSD, DARR, SPC5, and TOBSY spectra shown in Supplemental Fig. 3. To correct for relaxation during the mixing time, we compared the cross peak intensities to the diagonal peak of a 2D spectrum without any ^{13}C–^{13}C mixing. The result of this analysis, separated in overall transfer efficiency, transfer efficiency within the aliphatics, and from the aliphatics to the carbonyls and aromatic side chains, is shown in Table 1. The RFDR and DONER sequence show the highest overall (Cα – side chain + Cα–C′) transfer efficiencies and also the highest cross peak intensity for the Cα–C′ region of the spectrum. DREAM, on the other hand, proved to be the best sequence for magnetization transfer within the aliphatic region being twice as efficient as all the other sequences tested. Repeating this analysis for δ_1 slices other than 54 ppm led to essentially the same results given in Table 1 (data not shown).

Both the hard pulsed TOBSY and the adiabatic TOBSY showed low transfer efficiencies in our experiments. This can be explained

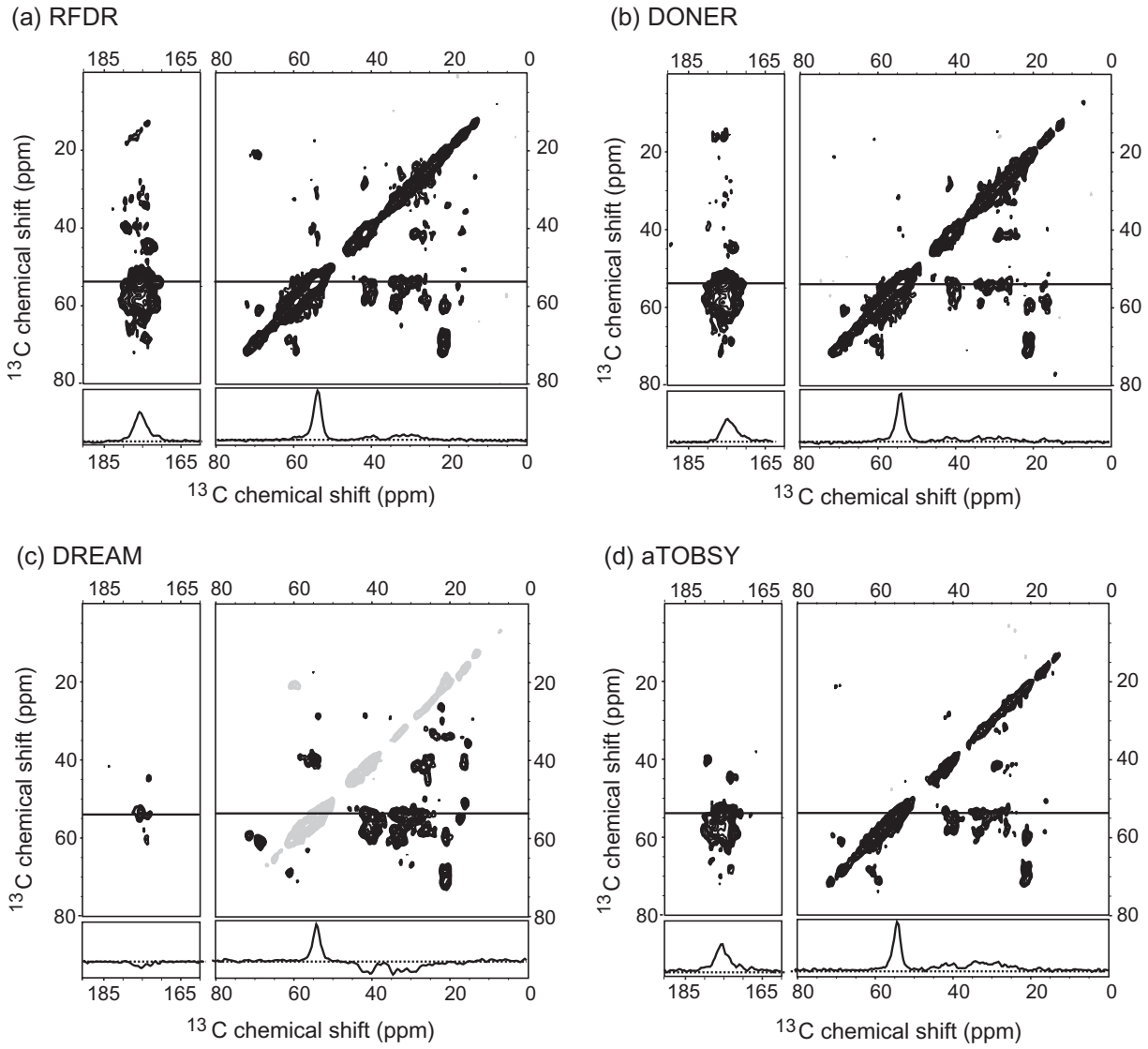

Fig. 1. 2D ^{13}C–^{13}C correlation spectra of perdeuterated ubiquitin microcrystals recorded with different ^{13}C recoupling sequences at 400 MHz. 1D slices, cut at δ_1 = 54 ppm, are shown below the corresponding 2D spectra. (a) RFDR, (b) DONOR, (c) DREAM, and (d) adiabatic TOBSY. RFDR, DONER, and adiabatic TOBSY spectra show strong Cα–C′ and relatively weak peaks between Cα and the side chain carbons. The DREAM spectrum, on the other hand, shows intense Cα to aliphatic cross peaks and less intense Cα–C′ correlations.

Table 1
Comparison of transfer efficiencies of different recoupling sequences based on the 1D slice corresponding to δ_1 of 54 ppm (Fig. 1). The total transfer efficiencies as well as the transfer efficiencies from Cα to C′, the side chain (aliphatic), and aromatic carbons are given. All transfer efficiencies are calculated as % of the diagonal peak at δ_1 of 54 ppm from a ^{13}C–^{13}C spectrum without mixing. RFDR generated the highest overall transfer efficiency but led, as most of the other sequences, primarily to strong Cα–C′ peaks. DREAM on the other hand proved to be more than twice as efficient for the aliphatic carbons as all the other sequences. Therefore, DREAM is the pulse sequence of choice if high transfer between Cα and other aliphatic carbons such as side chain carbons is needed.

Pulse sequence	Total transfer efficiency (%)	Transfer to C′ (%)	Transfer to aliphatic (%)	Transfer to aromatic (%)
RFDR	48 (±4)	33 (±1)	14 (±2)	1 (±1)
DONER	42 (±4)	26 (±1)	14 (±2)	2 (±1)
DARR	38 (±4)	25 (±1)	13 (±2)	–
PDSD	19 (±4)	9 (±1)	10 (±2)	–
TOBSY	29 (±4)	22 (±1)	7 (±2)	–
aTOBSY	31 (±4)	18 (±1)	13 (±2)	–
SPC5	16 (±4)	8 (±1)	8 (±2)	–
DREAM	37 (±4)	4 (±1)	33 (±2)	–

by the strong relaxation during the mixing time of the TOBSY sequence: TOBSY is a mostly $T_{1\rho}$ limited sequence because of the longer optimal mixing times required by the relatively weak J-coupling. Therefore, we observed a stronger overall magnetization decay during the TOBSY mixing than for DREAM and the T_1 limited sequences RFDR and DONER. This explains why the TOBSY and aTOBSY sequence give only 25% overall transfer efficiency when the transfer efficiency is calculated as described above. (In contrast, if we compared the transfer between cross peaks and diagonal within the same spectrum, *i.e.* without relaxation correction, we would obtain apparent transfer efficiencies of 71% and 61% for TOBSY and aTOBSY, respectively.) The SPC5 sequence also showed low absolute transfer efficiency because most of the magnetization decayed during the mixing time (if we compared the transfer between cross peaks and diagonal within the same spectrum, we would obtain apparent transfer efficiencies of 69%). Similar magnetization losses during continuous phase modulated, *i.e.* C and R-type, mixing sequences have been observed by others [37]. These magnetization losses probably come from pulse imperfections and could be instrument dependent.

All 2D spectra shown in Fig. 1 are asymmetric because we used ^{1}H–^{13}C CP as preparation sequence. CP leads to strong Cα, C′ magnetization at short contact times since these are the carbon spins closest to the only proton source, the amide protons. The Cβ peaks are stronger than Cγ, Cδ peaks due to the same reason. During the mixing time, magnetization mainly transfers from C′ to Cα and side chain carbons, and also from Cα to C′ and the side chain carbons, but not from the side chain carbons causing an asymmetric appearance of the spectrum. DREAM spectra are also inherently asymmetric even at equal carbon magnetization at the beginning of the recoupling [38]. Therefore, the DREAM spectrum in Fig. 1 is clearly asymmetric. Nevertheless, virtually all of the cross peaks are present on one side of the diagonal or the other, when compared with a 2D spectrum taken by Zech and co-workers on protonated ubiquitin [39] (with only a very few Val, Leu, and Ile Cγ and Cδ cross peaks as exceptions, see Supplemental Fig. 4).

The data presented above show that, generally, perdeuteration permits ^{13}C–^{13}C mixing without the need of ^{1}H or ^{2}H decoupling at relatively low MAS frequencies with high efficiency. To further prove this point, we recorded a DREAM spectrum with and without high-power ^{1}H decoupling during the DREAM recoupling step. As can be seen in Fig. 2, both spectra look essentially the same. The transfer efficiency within the aliphatics, and from the aliphatics to the carbonyls at δ_1 slice at 54 ppm decrease about 1% each. This similarity in transfer efficiency is a remarkable result considering that ^{1}H–^{13}C cross polarization still gives a higher signal than direct ^{13}C excitation, *i.e.* ^{1}H–^{13}C dipolar couplings are present in our sample.

The results obtained on a 400 MHz spectrometer appear to translate well to higher fields, as illustrated with RFDR and DREAM spectra collected at 750 MHz and 14 kHz MAS shown in Fig. 3. The overall transfer profile is the same under these conditions: RFDR leads to broadband mixing and relatively strong Cα–C′ cross peaks, DREAM leads to very high transfer efficiency in the aliphatic region of the spectrum.

Residual ^{1}H and ^{2}H couplings during t_1 and t_2 could influence the linewidths of the peaks in these spectra. Nevertheless, as can be seen from Supplemental Figs. 5 and 6 neither ^{1}H nor ^{2}H decoupling, nor the decoupling of both ^{1}H and ^{2}H had a relevant influence on the linewidth of our spectra. These results are similar to the results of Morcombe and co-workers [11], who recorded high-resolution spectra of perdeuterated ubiquitin without the need of any ^{1}H nor ^{2}H decoupling at a ^{1}H Larmor frequency of 800 MHz and 20 kHz MAS.

In summary, except for PDSD and DARR, *i.e.* sequences which essentially rely on the presence of a dense ^{1}H bath, all sequences perform well on perdeuterated proteins and show similar magnetization transfer patterns as when applied to fully protonated samples. RFDR, among the most robust and easy to set up pulse sequences tested, showed the highest overall transfer efficiency. However, broad banded mixing sequences typically lead to an accumulation of magnetization at the end of carbon chains [16] and, therefore, to strong Cα–C′ cross peaks. This can be a problem since strong Cα–C′ cross peaks lower the sensitivity of Cα-side chain cross peaks, which are often the main focus of the investigation especially when the Cα–C′ cross peaks are unresolved. The Cα-side chain cross peaks are often better resolved than Cα-C′ cross peaks and contain important information about secondary structure. DREAM is the mixing sequence of choice to get the most intense Cα-side chain cross peaks since it has by far the highest transfer efficiency in the aliphatic region of the spectrum. The negative cross peaks associated with the double quantum transfer make DREAM straight forward to optimize in a 1D version of the experiment. The high performance of the DREAM sequence is particularly noteworthy since a spin-lock field as low as ~4 kHz at the HORROR condition was employed without dramatic magnetization decay. Furthermore, the DREAM recoupling was not limited to the aliphatic region, but also clear Cα–C′ cross peaks were present in the spectra recorded at 400 MHz. Therefore, the combination of perdeuteration with the DREAM sequence makes it possible to record intense, low power 2D ^{13}C–^{13}C correlation spectra at moderate MAS frequencies. Moreover, only a double-resonance probe was used at 400 MHz and potentially a single channel probe could be used.

What is the prospect of these results at high MAS frequencies? DREAM was shown to work especially well at high MAS frequencies extending its recoupling bandwidth to the entire ^{13}C chemical shift range [29]. Furthermore, both DREAM and RFDR were shown to perform well without the need of ^{1}H decoupling at high MAS frequencies even on fully protonated samples [30,31]. We expect

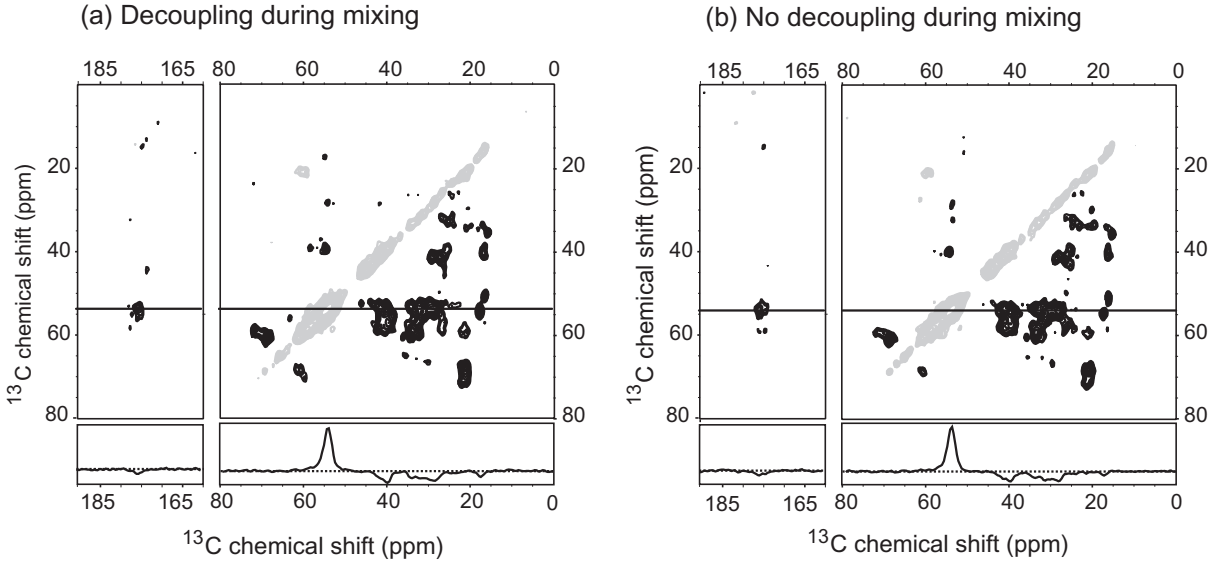

Fig. 2. 2D DREAM ^{13}C–^{13}C correlation spectra of perdeuterated ubiquitin microcrystals at 400 MHz. (a) Spectrum recorded with 95 kHz CW proton decoupling during DREAM mixing. (b) Spectrum recorded without proton decoupling. Note that the transfer efficiency is similar (check 1D slice at δ_1 = 54 ppm) and the transfer pattern is relatively complete in both spectra. This figure shows that high-power proton decoupling during the DREAM mixing time is not necessary for perdeuterated proteins.

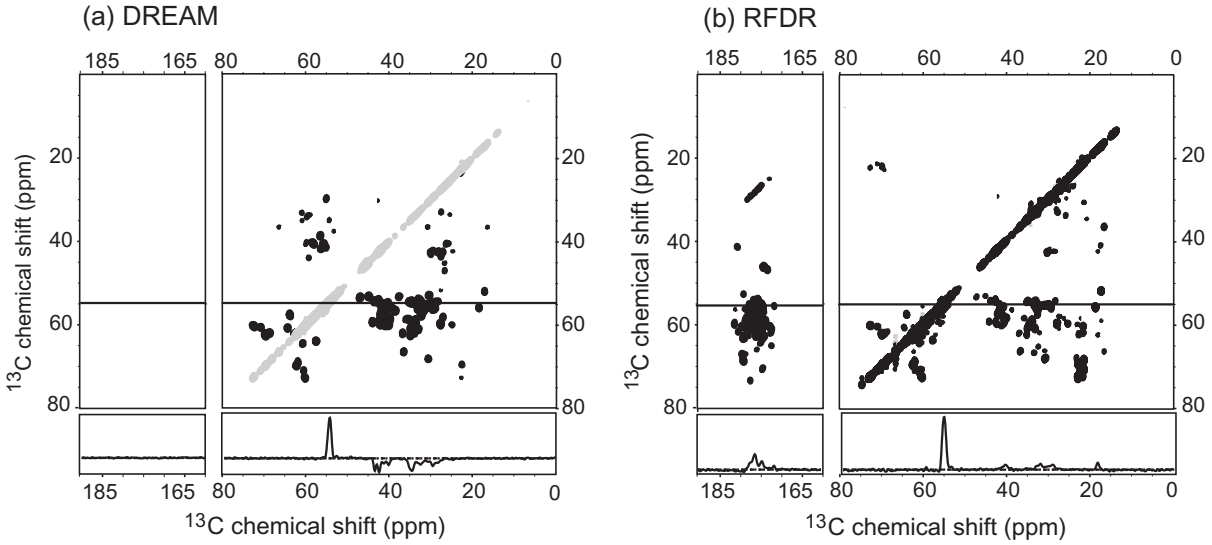

Fig. 3. 2D DREAM (a) and RFDR (b) ^{13}C–^{13}C correlation spectra of perdeuterated ubiquitin microcrystals recorded on a Bruker 750 MHz spectrometer. The transfer efficiency is good and the transfer pattern is relative complete in the case of both sequences. In that respect the result is very similar compared to the data recorded at 400 MHz. On the other hand the resolution is superior as expected and comparable to spectra recorded on fully protonated ubiquitin under high-power proton decoupling at 750 MHz (see Supplemental Fig. 4).

DREAM and RFDR to work equally well on perdeuterated samples under the same conditions. In this manuscript we showed that fast MAS is not essential, and that perdeuteration and slow MAS constitute a good alternative to fast MAS, since they permit high-resolution 2D spectra with good transfer efficiencies and without sample heating due to MAS or high-power ^{1}H decoupling.

3. Conclusions

Apart from proton assisted pulse sequences such as DARR and PDSD all homonuclear mixing sequences tested, performed very well on perdeuterated ubiquitin at relatively modest MAS frequencies and without any ^{1}H and ^{2}H decoupling. Therefore, perdeuteration makes it possible to record high quality 2D homonuclear correlation spectra with virtually no sample heating coming from MAS or ^{1}H decoupling.

We found that RFDR showed the highest overall transfer efficiency and DREAM gave the most intense cross peaks in the aliphatic region of the spectrum. Both sequences are robust and easy to setup and, therefore, form a very good alternative to DARR for perdeuterated samples.

4. Experimental

4.1. NMR

Solid-state NMR spectra at 400 MHz were recorded on a Varian Infinityplus spectrometer. DREAM and RFDR were performed using a 4 mm Apex (Chemagnetics) probe. For all the other sequences, we used a 4 mm T3 probe. Depending on the pulse sequence, samples were spun at a MAS frequency of 8 kHz or 8.333 kHz. The sample temperature was ~2 °C (set temperature = 0 °C). The CP rf-field strengths for all pulse sequences were 50 and 58 kHz for ^{13}C and ^{1}H, respectively, with a contact time of 1 ms. ^{13}C and ^{1}H hard-pulses were done with rf-field strengths of 50 and 100 kHz, respectively. The amplitude of the DREAM sweep was approximately 4 kHz (shape parameters: $\beta/2\pi$ = 1.4 kHz, $\Delta/2\pi$ = 0.7 kHz following [40]) and the mixing time was 2 ms. The RFDR mixing time was 3 ms. The DONER sequence follows the conditions described by Akbey and co-workers: ^{1}H and ^{2}H were irradiated simultaneously using a rotary resonance condition ($\omega_{1H} = \omega_{2H}$ = 8 kHz). The mixing time for DONER, DARR, and PDSD sequences was 50 ms.

The non-adiabatic TOBSY was recorded using a Post $C9^1_3$ mixing sequence with 8.333 kHz MAS, a ^{13}C rf-field strength of 50 kHz, and a mixing time of 7.5 ms [23]. The adiabatic TOBSY was recorded using a Wurst inverse Wurst (WiW) $C9^1_{18}$ mixing sequence with 8.333 kHz MAS and a mixing time of 4.3 ms [25]. The 120 μs long Wurst pulses were done with an exponent of q = 9, and a maximum rf-field strength of 70 kHz. As for the other sequences, no ^{1}H decoupling was applied during the TOBSY mixing.

The SPC5 spectrum was recorded with 8 kHz MAS using a ^{13}C rf-field strength of 40 kHz and a mixing time of 1 ms [16].

The spectral width was 40 kHz in both the direct and indirect dimensions, and 512 and 300 points were acquired in the t_1 and t_2 dimensions, respectively. No ^{1}H and ^{2}H decoupling was employed during t_1 and t_2.

The high-resolution 2D DREAM, and 2D RFDR spectra (shown in Fig. 3 and Supplemental Figs. 4 and 5) were recorded on a Bruker 750 MHz Advance II spectrometer using a 4 mm triple resonance HXY probe operating at 14 kHz MAS. The CP rf-field strengths for all the pulse sequences were 40 and 54 kHz for ^{13}C and ^{1}H, respectively and the contact time of the CP was 1 ms. ^{13}C and ^{1}H hard-pulses were performed with rf-field strengths of 40 and 100 kHz, respectively. The amplitude of the DREAM sweep was approximately 7 kHz and the mixing time was 2 ms. The RFDR mixing time was 3 ms. The spectral width was 94 kHz in both the direct and indirect dimension, and 2048 and 768 points were acquired in the t_1 and t_2 dimensions, respectively. For some of the spectra waltz decoupling of 5 kHz on ^{1}H and 2.5 kHz on ^{2}H was applied during t_1 and t_2. No decoupling was applied during the ^{13}C mixing sequences.

NMR spectra were processed and analyzed using the following programs: NMRPipe, SPARKY, SciPy.

4.2. Protein expression

The expression of uniformly ^{2}H, ^{13}C, and ^{15}N labeled ubiquitin was done following a protocol similarly to the one described by Tugarinov and co-workers except that *Escherichia coli* cells were slowly adapted to deuterated M9 minimal medium by going from a starter culture in 50 ml LB, 0% D_2O into a sequence of M9 minimal

media containing varying amounts of D_2O: 350 ml 0% D_2O, 2 l 70% D_2O, and 1 l 97–99% D_2O. After the expression, ubiquitin was purified as follows: The cell pellet was redissolved in 20 ml glacial acetic acid. The cell lysate was centrifuged at 4000*g* for 1 h. The supernatant of this spin was neutralized to pH ~5 with addition of 5 M KOH. This solution was then dialyzed twice against deionized water and a third time against 50 mM pH 4.5 ammonium acetate solution. The cell lysate was loaded onto a SP Sepharose column equilibrated with 50 mM ammonium acetate, pH 4.5 and eluted with 50 mM ammonium acetate, pH 5.5. Purity and labeling degree of ubiquitin was confirmed by mass spectrometry. Purified ubiquitin was crystallized at 4 °C by a batch method in 51% 2-methyl-2,4-pentanediol (MPD), 10% ethylene glycol, and 20 mM citrate buffer, pH 4.0–4.2. Protonated buffers and solutions were used during purification (including a protein unfolding step) and crystallization, leading to an essentially complete introduction of protons in all amides and exchangeable side chain moieties.

Acknowledgments

We thank Boris Itin for technical assistance in the NMR data collection. This work was supported by the following Grants NSF MCB 0316248 and NIH R01 GM 88724.

Appendix A. Supplementary material

Supplementary data associated with this article can be found, in the online version, at doi:10.1016/j.jmr.2010.10.015.

References

[1] E.K. Paulson, C.R. Morcombe, V. Gaponenko, B. Dancheck, R.A. Byrd, K.W. Zilm, Sensitive high resolution inverse detection NMR spectroscopy of proteins in the solid state, J. Am. Chem. Soc. 125 (2003) 15831–15836.
[2] B. Reif, B.J. van Rossum, F. Castellani, K. Rehbein, A. Diehl, H. Oschkinat, Characterization of 1H–1H distances in a uniformly 2H, 15N-labeled SH3 domain by MAS solid-state NMR spectroscopy, J. Am. Chem. Soc. 125 (2003) 1488–1489.
[3] V. Chevelkov, K. Faelber, A. Diehl, U. Heinemann, H. Oschkinat, B. Reif, Detection of dynamic water molecules in a microcrystalline sample of the SH3 domain of α-spectrin by MAS solid-state NMR, J. Biomol. NMR 31 (2005) 295–310.
[4] V. Agarwal, A. Diehl, N. Skrynnikov, B. Reif, High resolution 1H detected 1H, 13C correlation spectra in MAS solid-state NMR using deuterated proteins with selective 1H, 2H isotopic labeling of methyl groups, J. Am. Chem. Soc. 128 (2006) 12620–12621.
[5] R. Linser, U. Fink, B. Reif, Proton-detected scalar coupling based assignment strategies in MAS solid-state NMR spectroscopy applied to perdeuterated proteins, J. Magn. Reson. 193 (2008) 89–93.
[6] N.P. Wickramasinghe, M. Kotecha, A. Samoson, J. Past, Y. Ishii, Sensitivity enhancement in 13C solid-state NMR of protein microcrystals by use of paramagnetic metal ions for optimizing 1H T1 relaxation, J. Magn. Reson. 184 (2007) 350–356.
[7] N. Bloembergen, On the interaction of nuclear spins in a crystalline lattice, Physica 15 (1949) 386–426.
[8] K. Takegoshi, S. Nakamura, T. Terao, 13C–1H dipolar-assisted rotational resonance in magic-angle spinning NMR, Chem. Phys. Lett. 344 (2001) 631–637.
[9] I. Scholz, M. Huber, T. Manolikas, B.H. Meier, M. Ernst, MIRROR recoupling and its application to spin diffusion under fast magic-angle spinning, Chem. Phys. Lett. 460 (2008) 278–283.
[10] G. De Paëpe, J.R. Lewandowski, A. Loquet, A. Böckmann, R.G. Griffin, Proton assisted recoupling and protein structure determination, J. Chem. Phys. 129 (2008) 245101.
[11] C.R. Morcombe, V. Gaponenko, R.A. Byrd, K.W. Zilm, 13C CPMAS spectroscopy of deuterated proteins: CP dynamics, line shapes, and *T*1 relaxation, J. Am. Chem. Soc. 127 (2005) 397–404.
[12] V. Agarwal, B. Reif, Residual methyl protonation in perdeuterated proteins for multi-dimensional correlation experiments in MAS solid-state NMR spectroscopy, J. Magn. Reson. 194 (2008) 16–24.
[13] U. Akbey, H. Oschkinat, B. van Rossum, Double-nucleus enhanced recoupling for efficient 13C MAS NMR correlation spectroscopy of perdeuterated proteins, J. Am. Chem. Soc. 131 (2009) 17054–17055.
[14] V. Ladizhansky, Homonuclear dipolar recoupling techniques for structure determination in uniformly 13C-labeled proteins, Solid State Nucl. Magn. Reson. 36 (2009) 119–128.
[15] Y.K. Lee, N.D. Kurur, M. Helmle, O.G. Johannessen, N.C. Nielsen, M.H. Levitt, Efficient dipolar recoupling in the NMR of rotating solids. A sevenfold symmetric radiofrequency pulse sequence, Chem. Phys. Lett. 242 (1995) 304–309.
[16] M. Hohwy, C.M. Rienstra, C.P. Jaroniec, R.G. Griffin, Fivefold symmetric homonuclear dipolar recoupling in rotating solids: application to double quantum spectroscopy, J. Chem. Phys. 110 (1999) 7983.
[17] M. Baldus, D.G. Geurts, B.H. Meier, Broadband dipolar recoupling in rotating solids: a numerical comparison of some pulse schemes, Solid State Nucl. Magn. Reson. 11 (1998) 157–168.
[18] Y. Ishii, J. Ashida, T. Terao, 13C–1H dipolar recoupling dynamics in 13C multiple-pulse solid-state NMR, Chem. Phys. Lett. 246 (1995) 439–445.
[19] B.Q. Sun, C.M. Rienstra, P.R. Costa, J.R. Williamson, R.G. Griffin, Others, 3D 15N–13C–13C chemical shift correlation spectroscopy in rotating solids, J. Am. Chem. Soc. 119 (1997) 8540–8546.
[20] A.E. Bennett, R.G. Griffin, J.H. Ok, S. Vega, Chemical shift correlation spectroscopy in rotating solids: radio frequency-driven dipolar recoupling and longitudinal exchange, J. Chem. Phys. 96 (1992) 8624.
[21] A. Brinkmann, M. Edén, M.H. Levitt, Synchronous helical pulse sequences in magic-angle spinning nuclear magnetic resonance. Double quantum recoupling of multiple-spin systems, J. Chem. Phys. 112 (2000) 8539.
[22] M. Carravetta, M. Edén, X. Zhao, A. Brinkmann, M.H. Levitt, Symmetry principles for the design of radiofrequency pulse sequences in the nuclear magnetic resonance of rotating solids, Chem. Phys. Lett. 321 (2000) 205–215.
[23] E.H. Hardy, R. Verel, B.H. Meier, Fast MAS total through-bond correlation spectroscopy, J. Magn. Reson. 148 (2001) 459–464.
[24] M. Baldus, B.H. Meier, Total correlation spectroscopy in the solid state. The use of scalar couplings to determine the through-bond connectivity, J. Magn. Reson. A 121 (1996) 65–69.
[25] E.H. Hardy, A. Detken, B.H. Meier, Fast-MAS total through-bond correlation spectroscopy using adiabatic pulses, J. Magn. Reson. 165 (2003) 208–218.
[26] J. Leppert, B. Heise, O. Ohlenschläger, M. Görlach, R. Ramachandran, Broadband RFDR with adiabatic inversion pulses, J. Biomol. NMR 26 (2003) 13–24.
[27] R. Verel, M. Baldus, M. Ernst, B.H. Meier, A homonuclear spin-pair filter for solid-state NMR based on adiabatic-passage techniques, Chem. Phys. Lett. 287 (1998) 421–428.
[28] R. Verel, M. Ernst, B.H. Meier, Adiabatic dipolar recoupling in solid-state NMR: the DREAM scheme, J. Magn. Reson. 150 (2001) 81–99.
[29] M. Ernst, A. Detken, A. Bockmann, B.H. Meier, NMR spectra of a microcrystalline protein at 30 kHz MAS, J. Am. Chem. Soc. 125 (2003) 15807–15810.
[30] M. Ernst, M.A. Meier, T. Tuherm, A. Samoson, B.H. Meier, Low-power high-resolution solid-state NMR of peptides and proteins, J. Am. Chem. Soc. 126 (2004) 4764–4765.
[31] M.J. Bayro, R. Ramachandran, M.A. Caporini, M.T. Eddy, R.G. Griffin, Radio frequency-driven recoupling at high magic-angle spinning frequencies: homonuclear recoupling sans heteronuclear decoupling, J. Chem. Phys. 128 (2008) 052321.
[32] J.A. Stringer, C.E. Bronnimann, C.G. Mullen, et al., Reduction of RF-induced sample heating with a scroll coil resonator structure for solid-state NMR probes, J. Magn. Reson. 173 (2005) 40–48.
[33] C.V. Grant, C.H. Wu, S.J. Opella, Probes for high field solid-state NMR of lossy biological samples, J. Magn. Reson. 204 (2010) 180–188.
[34] G. De Paëpe, M.J. Bayro, J. Lewandowski, R.G. Griffin, Broadband homonuclear correlation spectroscopy at high magnetic fields and MAS frequencies, J. Am. Chem. Soc. 128 (2006) 1776–1777.
[35] Y. Mou, J.C.H. Chao, J.C. Chan, Efficient spin–spin scalar coupling mediated C-13 homonuclear polarization transfer in biological solids without proton decoupling, Solid State Nucl. Magn. Reson. 29 (2006) 278–282.
[36] C. Hughes, Radio-frequency driven polarization transfer without heteronuclear decoupling in rotating solids, Chem. Phys. Lett. 385 (2004) 435–440.
[37] M.J. Bayro, M. Huber, R. Ramachandran, et al., Dipolar truncation in magic-angle spinning NMR recoupling experiments, J. Chem. Phys. 130 (2009) 114506.
[38] A. Siemer, C. Ritter, M. Steinmetz, M. Ernst, R. Riek, B. Meier, 13C, 15N resonance assignment of parts of the HET-s prion protein in its amyloid form, J. Biomol. NMR 34 (2006) 75–87.
[39] S.G. Zech, A.J. Wand, A.E. McDermott, Protein structure determination by high-resolution solid-state NMR spectroscopy: application to microcrystalline ubiquitin, J. Am. Chem. Soc. 127 (2005) 8618–8626.
[40] A. Detken, E. Hardy, M. Ernst, et al., Methods for sequential resonance assignment in solid, uniformly 13C, 15N labelled peptides: quantification and application to antamanide, J. Biomol. NMR 20 (2001) 203–221.